

## **CHARACTERISING THE FAILURE AND REPOSE ANGLES OF IRREGULARLY SHAPED THREE-DIMENSIONAL PARTICLES USING DEM**

**Stuart R. MEAD<sup>1</sup>, Paul W. CLEARY<sup>1\*</sup> and Geoff K. Robinson<sup>1</sup>**

<sup>1</sup> CSIRO Mathematics, Informatics and Statistics, Clayton, Victoria 3169, AUSTRALIA

\*Corresponding author, E-mail address: Paul.Cleary@csiro.au

### **ABSTRACT**

In this paper we characterise the effects of many factors on the critical angles of a surface of granular material using the discrete element method (DEM). Factors investigated are the particle attributes (aspect ratio, angularity and particle size distribution) and the inter-particle contact friction. Fitted response surfaces to the friction and repose angles are used to determine the most significant factors controlling the critical angles and investigate the relationships between them.

### **INTRODUCTION**

Characterising the strength of a granular material is important in the food, minerals and processing industries for determining static (e.g. stable slope of material piles) and dynamic (e.g. milling, segregation) behaviour. In most cases, angles of repose and failure are readily measured. However, these properties represent the strength of the bulk granular material and do not fully convey details on the particle-scale properties that determine its strength. The critical angles are controlled by the characteristics of the individual particles that make up the granular material. In particular, particle shape (aspect ratios, angularity), size, contact friction and the range of variation in these properties all have some influence on the overall strength of the granular material and therefore on the critical angles.

The basic effects of particle shape were first demonstrated numerically by Gallas and Sokolowski (1993). Debroux and Cleary (2001), using the discrete element method (DEM), presented the effects of shape, size and friction on the critical angles in two dimensions. They represented the particles as two dimensional super-quadratics (SQ's) which can be used to represent a wide range of particle shapes and capture most of the essential features of natural grains. Using a slowly rotating cylinder 30% filled with non-round particles, they investigated the effect of the aspect ratio and angularity of grains on the critical angles. They found an increase in the angle of repose as the particle shape changed from circular to square. The effect of the particle aspect ratio on the critical angles was found to be far more complex than suggested by experimental work of Friedman and Robinson (2002). The critical angles increased with the aspect ratio until reaching a maximum angle at an aspect ratio of 2:1. As the aspect ratios increased beyond 2:1, the critical angles decreased significantly. This appeared to result from preferential alignment of particles with their long axis aligned in the flow direction, allowing them to slide over each other more easily. Three-dimensional simulations also by

Debroux and Cleary (2001), found that the drum rotation rate needed to be smaller for the flow to be in the avalanching regime. Zhou et al. (2002) investigated the angle of repose of spherical shaped particles using DEM. They developed an equation to estimate the angle of repose as a function of the particle and wall friction coefficients, particle diameter and width of the domain. However, this equation is only valid for spheres, so has little applicability to real world materials where particles are typically not spherical. No previous studies have investigated the effect of three dimensional shaped particles on the critical angles.

The importance of particle shape in three dimensions was first highlighted using DEM by Cleary and Sawley (2002) in an investigation of discharge flows from hoppers. Cleary (2009) also provided examples of several industrial applications in which particle shape was found to be very important and gave an exposition of the role of particle shape and how it affects different types of particle flows. Owen et al. (2009) compared DEM predictions in 2D and 3D with experimental results for a quasistatic collapsing granular column. The experimental method used in their investigation can also be used to measure the critical angles. They found that it was necessary to both perform the modelling in 3D and to include particle shape in order to obtain reasonably accurate prediction of shear planes. The static particle microstructure in two-dimensional and three-dimensional spherical simulations was found to be too weak to correctly predict the slope failure and therefore the angle of repose.

These previous numerical and experimental studies of the critical angles have demonstrated the effects of particle attributes and mechanical properties on the critical angles. Missing from these previous investigations has been the determination of the relative importance and functional variation of each property on the critical angles. Knowledge of how and to what degree each attribute affects the critical angles can result in a better understanding of the strength of granular materials and potentially assist with the development of new models that predict the critical angles directly from particle properties. To better understand the influence of each characteristic, DEM simulations of three-dimensional shaped particles were performed. In this study we focused on the angle of repose obtained using a rotating cylinder in the avalanching regime. For a summary of bed regimes in a rotating cylinder, refer to Debroux and Cleary (2001). In the avalanching regime, the cylinder is rotated slowly and the free surface angle of the granular material increases up to the angle of failure before avalanching occurs along the free surface and the surface angle declines to the angle of

repose. This is a quasistatic or creeping process, with short duration discrete dynamic avalanches interrupting long periods of slow rigid body rotation by the bed. This pattern repeats allowing the collection of time series for the critical angles and an accurate estimation of their averages. Using a Box-Behnken experimental design, we explore the effects of the particle attributes (aspect ratio, angularity, size distribution) and the inter-particle friction on the repose and failure angles.

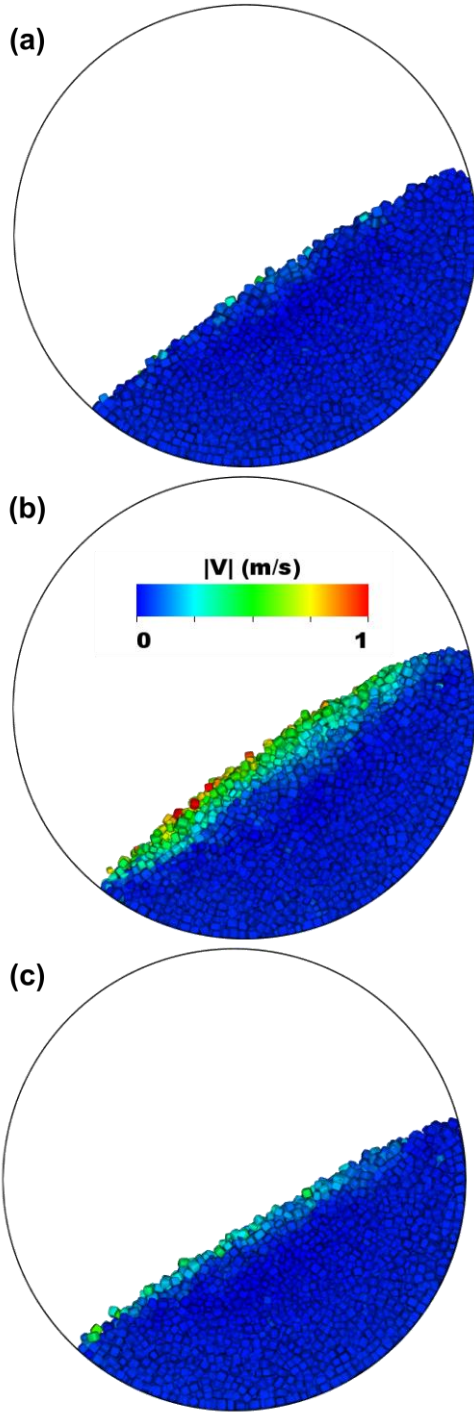


**Figure 1:** (a) the point of failure, (b) mid-way through the avalanche, and (c) as the avalanche comes to rest during a discrete avalanche in a slowly rotating cylinder.

## DEM CONFIGURATION AND SLOPE ANGLE CALCULATION

In this study, we use DEM to predict the critical angles of granular materials in a slowly rotating cylinder test. DEM is a meshless numerical method which is used to model granular materials at the particle scale. This implementation uses a linear spring-dashpot model, described in detail by Cleary (2004, 2009). The effects of particle shape characteristics are investigated by representing the particles as super-quadratics (SQ's), which have the general form:

$$\left(\frac{x}{a}\right)^m + \left(\frac{y}{b}\right)^m + \left(\frac{z}{c}\right)^m = 1 \quad (1)$$

The particle angularity is determined by the power  $m$ , with  $m = 2$  giving spherical particles and with the shape becoming cubic as  $m \rightarrow \infty$ . The aspect ratios are determined by the ratios of the semi-major axes ratios  $b/a$  and  $c/a$ .

A 1 m diameter cylinder was filled to 30% of its volume with particles. The mean length of the major axis for the particles was 25 mm. The coefficients of restitution for particle-particle and particle-wall collisions were 0.5 for all simulations. Initial tests showed little sensitivity to the specific value used. The flow and critical angles were also not sensitive to the spring stiffness provided it was higher than  $8 \times 10^3$  N/m. Average particle overlaps were approximately 0.5% for all simulations. The particle-wall friction coefficient was set to 0.9 so that there was good frictional contact between the bed and the cylinder, and no bulk sliding of the bed. The cylinder was modelled as axially periodic in order to eliminate the effect of any end walls. The periodic section depth was 0.5 m.

The cylinder revolution rate was 1 rpm so that the flow occurred as a series of discrete avalanches. Figure 1 displays a typical discrete avalanche. The angle of the free surface of the bed of granular material slowly increases until it reaches the angle of failure, shown in figure 1a. The slope then fails, causing an avalanche, shown half way through its motion in figure 1b. The particles then come to rest at the angle of repose, shown in figure 1c. The angle then slowly increases back to the angle of failure in a repeating process.

The instantaneous free surface angle of the material is calculated at regular time intervals in the DEM code and is used to determine the angles of failure and repose of the material. For a detailed description of the slope angle calculation method, refer to Debroux and Cleary (2001). Figure 2 displays the time variation of the slope angle of the granular bed in the avalanching regime. The peaks and troughs of the slope angle correspond to the failure and repose angles of discrete avalanche events.

The slope angle is smoothed using an exponential smoothing method, and is then used in the identification of the major peaks and troughs, which correspond to the failure and repose angles. The smoothed slope angle and major peaks and troughs are also shown in figure 2. The failure and repose angles are then calculated as the average of the identified peaks and troughs of the time series. The simulation is performed for sufficient time to obtain critical angles with very small standard deviations.

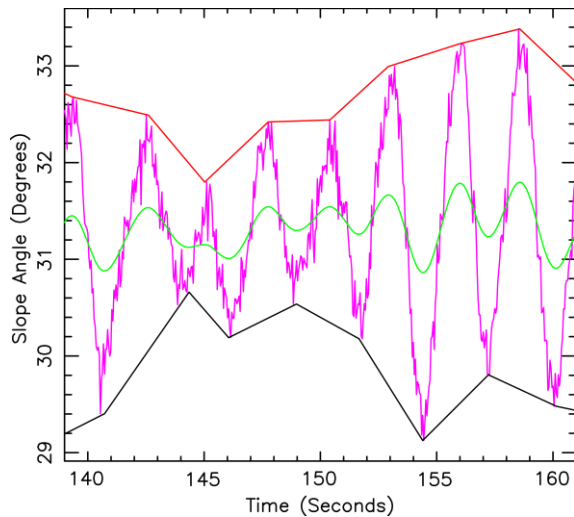


**Figure 2:** Major peaks (red) and troughs (black) in the slope angle (purple), the green line is the smoothed slope angle used to detect peaks and troughs.

### BOX-BEHNKEN EXPERIMENT

The variation of the critical angles was investigated using a 3 level, 4 factor Box–Behnken experimental design. Box-Behnken designs are a class of response surface experimental designs. They are used to describe the relationships between explanatory factors (e.g. particle properties) and the response variable (e.g. failure and repose angles) as a continuous fitted surface. In this Box-Behnken design, 27 experiments were run. Three of the runs were centre points (all factors held at their mid-values) with the remaining 24 being six small experiments in which two factors are kept at the mid-value while the other two factors are varied across their extreme values.

Since the aspect ratios of natural particles are generally not independent of each other and to reduce the variables in this initial study, we chose to investigate the two aspect ratios as one variable. This reduces the number of variables investigated to four. The four factors considered in this experiment were the width of the particle size distribution (PSD), the particle-particle friction ( $\mu_p$ ), the SQ angularity index ( $m$ ) and the aspect ratio (AR).

Table 1 shows the three levels of each factor investigated in the experiment.

- The three particle-particle friction values were chosen as the plausible minimum, median and maximum contact friction values possible for real materials.
- The SQ index was chosen to represent three different types of angularities seen in granular materials. The first level represents the most rounded natural particles likely to be found, such as river gravel. The second level represents the most common angularity range of natural particles, such as quartz sand. The third level represents the most extreme angularities found in granular materials, such as charcoal, briquettes or newly crushed rock.
- The aspect ratios represent three different classes of materials, which are likely to exhibit different behaviours. The first level (rounded) represents the most common particle aspect ratios found in crushed particles such as rocks. There is some difference in

the axes lengths, but there is no easily discernable major axis. The second level (intermediate) represents more plate-like particles such as shale, where one axis is markedly smaller than the other two. The third level (elongated) represents grain-shaped particles, such as rice or wheat, where there is one immediately apparent major axis, and two minor axes.

- The three PSD ranges, using a normal distribution by mass, of  $\pm 5$ , 25 and 50% of the mean particle diameter were chosen to represent near mono-dispersed, poly-dispersed and highly poly-dispersed distributions of particle sizes.

Level	$\mu_p$	$m$	AR	PSD
1	0.2	2.1-2.5	0.8 - 1.0, 0.6 - 1.0	$\pm 5\%$
2	0.4	2.4-3.5	0.8 - 1.0, 0.25 - 0.8	$\pm 25\%$
3	0.8	3.0-6.0	0.3 - 0.6, 0.25 - 0.5	$\pm 50\%$

**Table 1:** Three levels of particle-particle friction ( $\mu_p$ ), angularity ( $m$ ), aspect ratio class (AR) and particle size distribution (PSD) used in the experiment.

A response surface with linear, quadratic and cross-product terms was fitted to the angles of failure and repose. Estimates of the coefficients for the model fitted to failure angle are shown in table 2. The coefficient of determination ( $R^2$ ) for this model was 0.98 and the standard deviation of the residual was 0.49 degrees. This indicates a fairly accurate fit of the model to the experimental data.

Coefficients		Estimate
<b>Quadratic</b>	Friction	-1.57
	Angularity	0.51
	Aspect Ratio	1.15
	PSD	-1.38
<b>Linear</b>	Friction	3.32
	Angularity	1.57
	Aspect Ratio	0.70
	PSD	2.18
<b>Cross-Product</b>	Friction Angularity	-0.22
	Friction Aspect Ratio	2.56
	Friction PSD	0.36
	Angularity Aspect Ratio	-0.80
	Angularity PSD	-0.18
	Aspect Ratio PSD	1.91
<b>Intercept</b>		28.39

**Table 2:** Coefficients for the fitted model of the failure angle.

The derivative of the fitted model in the centre of the experimental region provides a simple summary of the

relationships. For this model, the derivatives are 3.32, 1.57, 0.7 and 2.18 for friction, angularity, aspect ratio and PSD respectively. The derivatives show that increasing the level from the centre point will result in an increase in the failure angle. Contact friction and PSD cause the largest increases in the angle, with angularity causing moderate increases and aspect ratio having a relatively minor effect.

The statistical significance of the coefficients was tested. The main effects (squared and linear terms) of all factors were found to be important. Only the cross-product terms that included aspect ratio were statistically significant. This suggests there are no interactions between the effects of friction, angularity and PSD on the critical angles.

### INFLUENCE OF INDIVIDUAL FACTORS ON CRITICAL ANGLES

The main effects predicted by the response surface for failure angle are shown in figure 3. For each of the curves, all other factors were held at their centre values.

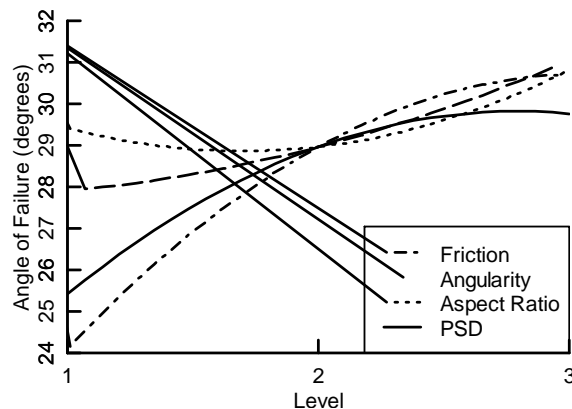


**Figure 3:** Angle of failure as a function of friction, angularity, aspect ratio and PSD. For each curve, all other factors are held at their centre level.

The friction coefficient (dash-dotted line) causes the largest change in the failure angle, rising from 24 degrees for a coefficient of 0.2 to 31 degrees for a coefficient of 0.8. Friction between contacting particles determines the ability of grains to slide against each other. In a quasi-static process such as the rotating cylinder test, sliding motion is likely to be most common. The coefficient of friction therefore has a large direct effect on the shear strength of the material, whereas the other particle properties indirectly affect the forces by modifying the number of contacts.

The angle of failure increases almost linearly by 3.0 degrees across the range of particle angularity (dashed line). The sharper corners of angular particles promote better interlocking between them. This results in a stronger particle microstructure with increasing the resistance to rotation and sliding. This increased resistance to motion is what causes the increasing failure angle.

The main effect of aspect ratio (dotted line) on the angle of failure is smaller than the main effects of the other factors. The failure angle lies between 28.9 and 30.5 degrees, and is lowest for the plate-like (intermediate) particles (aspect ratio 2). Debroux and Cleary (2001) also found (in 2D) that the angle of failure decreased for higher aspect ratio particles due to tendency for preferential

alignment of the grains parallel to their neighbours. The angle of failure is highest for the elongated particles (aspect ratio 3). This is caused by the lack of preferential alignment in the particle microstructure.

PSD breadth (solid line) has the second largest individual effect on the failure angle. It increases from 25.5 degrees to 29.5 degrees as the PSD breadth increases from 5% to 25%. The higher PSD means that particles can fill the gaps between larger particles better, which results in a higher number of contacts with neighbouring particles. An increase to the PSD from 25 to 50% resulted in much smaller increase in failure angle of 1 degree. This indicates that the effect of PSD breadth on the failure angle decreases as the particles become progressively more poly-disperse.

Fitted response curves of the repose and failure angles had similar features, with the repose angle being smaller by between 1 and 3 degrees. The largest difference between the main-effect curves was for the PSD, where the repose angle decreased slightly between 25 and 50%.

### INFLUENCE OF INTERACTIONS ON CRITICAL ANGLES

The fitted response surfaces indicated that only the interactions between the aspect ratio and the other factors were statistically significant. This means that the aspect ratio causes the effects of friction, angularity and PSD to vary. In contrast, choices of friction, angularity and PSD do not generate significantly different behaviours of these factors.

The effects of the interactions between aspect ratio and the remaining factors are shown in figures 4 to 6. They display contours of the angle of repose and failure at each level of aspect ratio for each factor of friction, angularity and PSD. The continuous lines are the failure angle and the dashed lines are the repose angle.

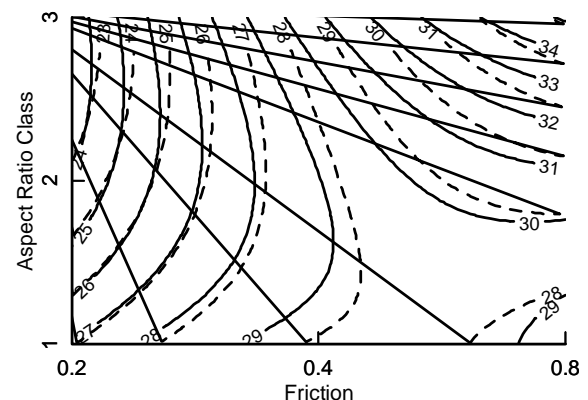


**Figure 4:** Contour lines of failure angle (solid line) and repose angle (dashed line) at each level of friction and aspect ratio with all other values are held at their centre level. The printed numbers on the contour lines represent the magnitude of the angle.

Figure 4 shows the interaction between aspect ratio and the friction coefficient. The critical angles tend to increase as friction increases from 0.2 to 0.8. The increase is most significant for the elongated particles (aspect ratio 3), but is less rapid for plate like particles (aspect ratio 2) and has little effect for friction coefficients higher than 0.6. For the rounded particles (aspect ratio 1), the angles increase

at a much slower rate with increasing friction and there is little change beyond a friction coefficient of 0.4. As the aspect ratio becomes more elongated (i.e. increasing from 1 to 3), the number of contacts between particles increases and the particles will tend to align with their long axis parallel to flow allowing sliding motion to become more pronounced. The increased number of contacts and sliding motion enables the friction to have a more pronounced effect on the granular strength.

Figure 5 shows the interaction between the aspect ratio and particle angularity. For elongated particles (aspect ratio 3), the angularity has only a small effect when changing between medium and high values and almost no effect when changing from low and medium values. The angularity has more of an effect for the intermediate aspect ratio particles. Increasing their angularity causes a more tightly packed and interlocked microstructure which results in greater resistance to motion. For the more rounded particles (aspect ratio 1), increases in angularity result in a consistent increase to the critical angles as the resistance to motion increases.

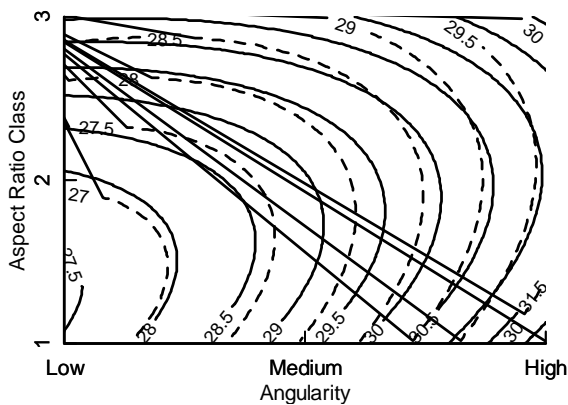


**Figure 5:** Contour lines of failure angle (solid line) and repose angle (dashed line) at each level of angularity and aspect ratio with all other values are held at their centre level. The printed numbers on the contour lines represent the magnitude of the angle.

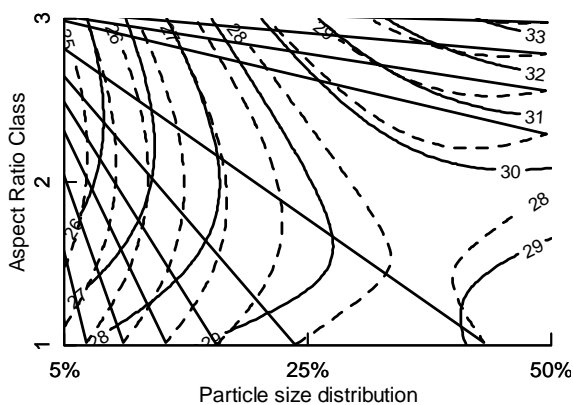


**Figure 6:** Contour lines of failure angle (solid line) and repose angle (dashed line) at each level of PSD and aspect ratio with all other values are held at their centre level. The printed numbers on the contour lines represent the magnitude of the angle.

The interaction between aspect ratio and PSD is displayed in figure 6. There is a much larger difference between failure and repose angles in this interaction compared to others. For the elongated particles (aspect ratio 3), the

PSD has a large effect on the angles. This effect is smaller for the intermediate and rounded particles, with a minor increase in the critical angles from 25% to 50% PSD. This means that the effect of PSD breadth on the failure angle decreases as the particles become more poly-disperse, but the magnitude of the effect decreases as the particles become more elongated. The effect of PSD reaches a maximum between a PSD breadth of 25 and 50% for rounded and intermediate particles, but is still increasing at 50% PSD for elongated particles.

## RELATIONSHIP BETWEEN FAILURE AND REPOSE ANGLES

When a quadratic response surface was fitted to the difference between the failure and repose angles, only two terms were statistically significant. The breadth of the PSD was the only main effect influencing the difference and this was only just significant. The strongest term was the interaction of the aspect ratio with the breadth of the PSD.

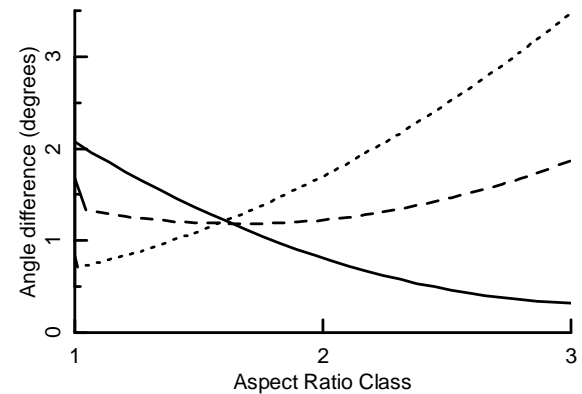


**Figure 7:** Difference between failure and repose angles with varying aspect ratio for PSD breadths of 5% (solid line), 25% (dashed line) and 50% (dotted line). Friction and angularity were kept at the centre value.

Figure 7 shows the difference between the failure and repose angles as a function of aspect ratio for the three different PSD breadths. For a PSD of 5% (solid line), the difference is highest for rounded particles, but decreases with increasing aspect ratio to less than 0.3 degrees for the most elongated ones. For a moderately poly-disperse PSD of 25% (dashed line), the difference between the angles is lowest for the intermediate aspect ratios and increases slightly for both rounded and elongated particles, remaining between 1 and 2 degrees. The highest difference occurs for the elongated particles, which is completely the opposite behaviour to the near mono-disperse particles. For the most poly-disperse particles with a PSD of 50% (dotted line), the difference is now only slightly non-linear but the gradient is now very high with the minimum occurring for the rounded particles and the maximum (of now more than three degrees) for the elongated particles. The changing aspect ratio now has the complete opposite effect on the difference than it had for near mono-disperse particles. The curves intersect at a moderate aspect ratio between the rounded and intermediate aspect ratio particles where the angle difference trends reverse.

The three dimensional response surface showing the dependence of the critical angle difference on aspect ratio and PSD is shown in figure 8. Following the rounded particles (aspect ratio class 1) along the PSD axis, the

angle difference decreases as the particles become more poly-disperse. The trend reverses for the intermediate aspect ratio particles, with the difference increasing as the PSD increases. For the elongated particles, the difference increases strongly as the particles become more poly-disperse. The largest angle difference is 3.5 degrees, for aspect ratio class 3 and 50% PSD.

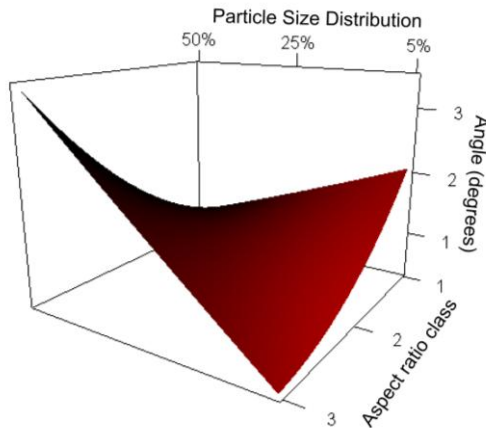


**Figure 8:** 3d response surface of the difference between failure angle and repose angle for variations in PSD and aspect ratio. The friction and angularity were held at the centre values.

## CONCLUSIONS

The angles of repose and failure of granular materials vary with mechanical (friction) and geometric properties (PSD, angularity and aspect ratio). Their relationships were investigated using DEM simulations of a rotating cylinder in the discrete avalanching regime. A Box-Behnken experimental design was used to explore the functional dependence of these parameters using a small number of combinations of tested conditions. Response surfaces with linear, quadratic and cross-product terms were fitted to the numerical data, with a coefficient of determination of 0.98 and standard deviation of the residuals of 0.49. The statistical significance of each coefficient was tested, which indicated that the main effects (squared and linear terms) of all factors were significant. Only the cross-product terms that included aspect ratio were statistically significant.

The friction had the strongest main effect on the critical angles. The other three factors of angularity, aspect ratio and PSD were important but had smaller magnitudes. The aspect ratio was found to cause the effects of friction, angularity and PSD to vary. For rounded particles, friction and PSD had relatively small and decreasing effects on the magnitude of the angle, whereas angularity had a much larger effect. Elongated particles exhibited the opposite behaviour, showing a high sensitivity to friction and PSD, but little to angularity. Intermediate aspect ratio particles exhibited similar behaviour to the more elongated particles, but the effects were less pronounced. They demonstrated a reasonable sensitivity to friction and PSD, and only a small sensitivity to angularity.

The difference between the failure and repose angles was sensitive only to the cross product between aspect ratio and PSD. The PSD as a main effect was also statistically

significant, but only to a small degree. Each aspect ratio exhibited a different response to the PSD. For rounded particles, the angle difference was highest for the near mono-disperse PSD and lowest for high poly-dispersity. For intermediate and elongated particles, the complete opposite effect was seen. The crossover point for the different behaviours occurred between the rounded and intermediate aspect ratio particles.

The existence of behaviours that can be fitted to such a model demonstrates the possibility of determining the particle-scale properties (that control bulk material strength) from simple bulk characterisation measurements. This information is useful to a variety of granular material handling industries where prediction and control of the material strength is required. The different behaviours shown in the fitted model can be used to narrow the range of combinations of particle properties that match the observed critical angles. This is particularly important for DEM simulation of complex particle flows where there is only bulk material information available for characterising the material, but which cannot be used directly in the specification of the DEM particles or their properties.

## REFERENCES

- BUCHHOLTZ, V. and PÖSCHEL, T., (1994), "Numerical investigations of the evolution of sandpiles." *Physica A: Statistical Mechanics and its Applications*, 202, 390-401.
- CLEARY, P. W., (1998), "Discrete element modelling of industrial granular flow applications" *TASK Quarterly*, 2.
- CLEARY, P. W. & SAWLEY, M. L., (2002), "DEM modelling of industrial granular flows: 3D case studies and the effect of particle shape on hopper discharge." *Appl. Math. Model.*, 26, 89-111.
- CLEARY, P. W., (2004) "Large scale industrial DEM modelling" *Eng. Computation.*, 21, 169 – 204.
- CLEARY, P. W., (2009) "Industrial particle flow modelling using discrete element method" *Eng. Computation.*, 26(6), 698 – 743.
- DEBROUX, F. AND CLEARY, P. W., (2001), "Characterising the angles of failure and repose of avalanching granular material using the DEM method", *Proc. 6<sup>th</sup> World Cong. of Chem. Eng.*
- FRIEDMAN, S. P. and ROBINSON, D. A., (2002), "Particle shape characterization using angle of repose measurements for predicting the effective permittivity and electrical conductivity of saturated granular media", *Water Resour. Res.*, 38, 1236.
- GALLAS, J. A. C. and SOKOŁOWSKI, S., (1993), "Grain non-sphericity effects on the angle of repose of granular material", *Int. J. of Mod. Phys. B*, 7, 2037-2046.
- OWEN, P. J., CLEARY, P. W. and MÉRIAUX, C., (2009), "Quasi-static fall of planar granular columns: comparison of 2D and 3D discrete element modelling with laboratory experiments", *Geomechanics and Geoengineering*, 4, 55-77.
- ZHOU, Y. C., XU, B. H., YU, A. B. and ZULLI, P., (2002), "An experimental and numerical study of the angle of repose of coarse spheres", *Powder Technology*, 125, 45-54.